Facile Synthesis of Ferrocene Biscrown Ethers and Ferrocene Cryptands: NMR Complexation Studies and the Redox-Switched Bonding of H^+ and Na^+

Herbert Plenio*[a], Hanaa El-Desoky[b], and Jürgen Heinze[b]

Institut für Anorganische und Analytische Chemie[a] and Institut für Physikalische Chemie[b], Universität Freiburg, Albertstraße 21, 79104 Freiburg, Germany

Received June 18, 1993

Key Words: Ferrocene / Crown ethers / Cryptands / Redox switching / Protonation

The reaction of 1,1'-ferrocenylene-bis(methylenepyridinium) tosylate chloride (**1**) with aza-x-crown-y (x/y = 12/4; 15/5; 18/6) gives the three novel ferrocene biscrown ethers 1,1'-ferrocenylene-bis(methylene-aza-x-crown-y) (x/y = 12/4, **2**; 15/5, **3**; 18/6, **4**). The reaction of **1** with diaza-18-crown-6 represents a new and simple route to the known ferrocene cryptands 1,1'-ferrocenylene-[bis-7,16-methylene(1,4,10,13-tetraoxa-7,16-diazacyclooctadecane)] (**5**) and 1,1'':1',1'''-bisferrocenylene-bis-[bis-7,16-methylene(1,4,10,13-tetraoxa-7,16-diazacyclooctadecane)] (**6**). The solid-state structure of **5** is described. The ferrocene bridge compresses the diaza crown ether leading to an internitrogen distance of 458 pm. The stoichiometry of Na^+ and K^+ complexes with **2** and **3** in CD_3CN determined in NMR titration experiments suggests the formation of Na^+ and K^+ crown ether sandwich complexes in solution. Cyclic voltammograms of **2** and **5** in the presence of varying amounts of H^+ and Na^+ have been recorded. The redox potential of ferrocene is shifted by +180 mV in the case of **5** · Na^+ and up to +600 mV in the case of **5** · H^+H^+ relative to **5**, but only by +70 mV with **2** · Na^+ and **2**. The protonation of **5** give rises to several isomers (*exo* and *endo* protonation) which differ significantly in their redox potential. The extremely large positive shift of the oxidation potential of the diprotonated ferrocene cryptand corresponds to an increase in the acidity of **5** · H^+H^+ upon oxidation by more than ten orders of magnitude and makes this system a candidate for the directed membrane transport of protons.

One of the most prominent molecules of organometallic chemistry is ferrocene, whose most characteristic features are the sandwich structure and its redox chemistry[1]. Crown ether ligands on the other hand are modern representatives of classic coordination chemistry, which are known to form exceptionally stable complexes with alkali metal ions[2].

Chemically linking ferrocene and crown ethers combines their specific properties. Thus, the reversibility of the ferrocene/ferrocenium redox couple and the high stability of crown ether metal complexes can cooperate within one molecule[3]. This synergetic relation creates a switch on a molecular level, which allows the complexing ability to be turned off (i.e. drastic decrease of the complexation stability constant) of the macrocyclic subcomponent, once a positive charge within the ferrocene moiety is generated. Upon reduction the ability for cation complexation is restored; consequently, the combination of ferrocene and crown ether produces a redox-switched crown ether[4].

Ferrocene macrocycles with a Fc(CON) amide structure were synthesized by Beer[5] and Hall[6]. The weak redox switching effect upon addition of monovalent cations suggested that coordination of metal ions does not occur within the macrocycle but rather on the periphery at the amide oxygen[7]. This was confirmed recently by the solid-state structure of a ferrocene cryptand with Dy^{3+} in which five of the seven coordination sites at dysprosium are occupied by four amide oxygen atoms and one water molecule[8]. Our target therefore was to synthesize ferrocene-containing macrocycles without the disadvantages of an amide structure. In this paper we report on a simple synthesis of new ferrocene biscrown ethers, an improved synthesis of ferrocene cryptands, and an investigation of the effects of H^+, Li^+, Na^+, and K^+ complexation on NMR spectra and the electrochemical behavior.

Results and Discussion

The salt 1,1'-ferrocenylene-bis(methylenepyridinium) tosylate chloride (**1**) is easily available from ferrocene in two steps[9] via 1,1'-Fc$(CH_2OH)_2$. This compound is the ideal starting material for the synthesis of ferrocene-biscrown ethers and ferrocene cryptands. The reactions of **1** with aza-12-crown-4, aza-15-crown-5, or aza-18-crown-6 in the presence of Na_2CO_3 afford the corresponding novel biscrown ethers **2**, **3**, and **4** in yields of 45–65%. The analogous reaction of **1** with diaza-18-crown-6 yields as the main product the known ferrocene cryptand[10] **5** and as a result of a 2 + 2 condensation the ferrocene cryptand **6** (Scheme 1). Compounds **2**, **5**, and **6** are orange-yellow solids, whereas **3** and **4** form highly viscous orange-red oils. This route is superior to the published ones for **5** and **6** as it is much shorter and also uses cheap starting materials[10,11].

Solid-State Structure of 5

The X-ray crystal structure of **5** displays the expected ferrocene-clamped arrangement of the 18-membered macro-

  0009–2940/93/1111–2403 $ 10.00+.25/0

Scheme 1. Synthesis of **2**, **5**, and **6**. a. aza-12-C-4, Na_2CO_3, b. diaza-18-C-6, Na_2CO_3, c. $NaBPh_4$ (M = Na)

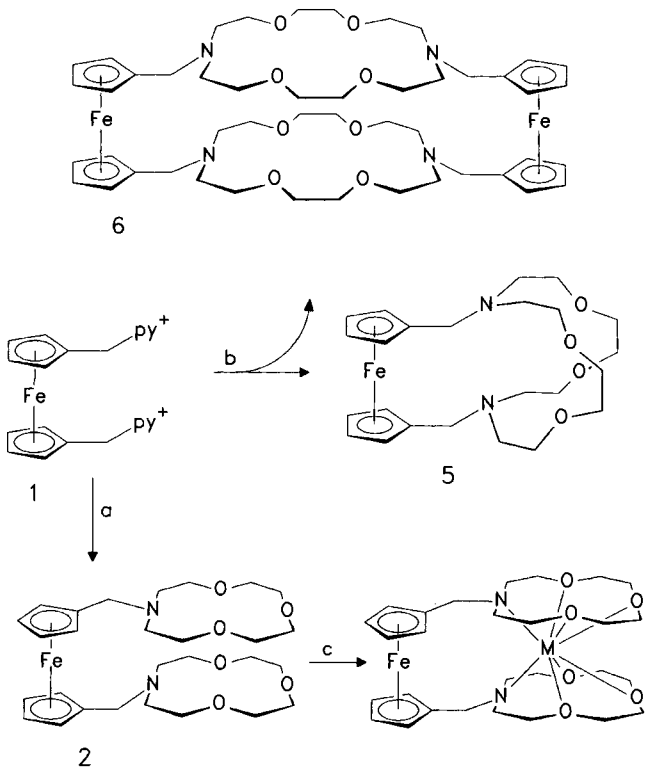

1,1′-Ferrocenylene-bis(methylene-aza-*x*-crown-*y*)

	2	3	4
x	12	15	18
y	4	5	6

cycle (Figure 1). The tilting of the planes of the two cyclopentadienyl rings of 4.6° and the torsion angle [C4–C5–C6–N1] = 175° effect a nitrogen-nitrogen distance of 458 pm and an elliptical distortion of the crown ether ring. This distortion becomes more apparent when compared with the corresponding internitrogen distance of 580 pm in diaza-18-crown-6[12]. A comparison of the structural data of **5** with **5** · H_2O[11] illustrates how sensitive bonding parameters respond to minor changes in the environment. The moderate tilt of the planes of the cyclopentadienyl rings in **5** as opposed to **5** · H_2O is obviously caused by different crystal packing forces and the coordinated water molecule. In **5** · H_2O the cyclopentadienyl rings are coplanar whereas the internitrogen distance is 550 pm. The substantially different nitrogen-nitrogen distances illustrate the limited value of solid-state structures for assessing the cavity size of crown ethers, thus requiring an investigation of the coordination behavior in solution.

NMR Spectra and Complexation of Cations in Solution

For a ^1H- and ^{13}C-NMR investigation of the coordination chemistry of the ferrocene biscrown ethers and the ferrocene cryptands the compounds are dissolved in CD_3CN and successively treated with $LiAsF_6$, $NaBPh_4$, or $KBPh_4$. The ^1H and ^{13}C resonances of the macrocycle and to a smaller extent those of the ferrocene are shifted until the complexation reaction is complete. This effect is more easily observed in the ^{13}C-NMR spectra, since the larger signal dispersion of the ^{13}C spectra amplifies the effects caused by salt addition. Consequently, some of the signals are shifted by up to 5

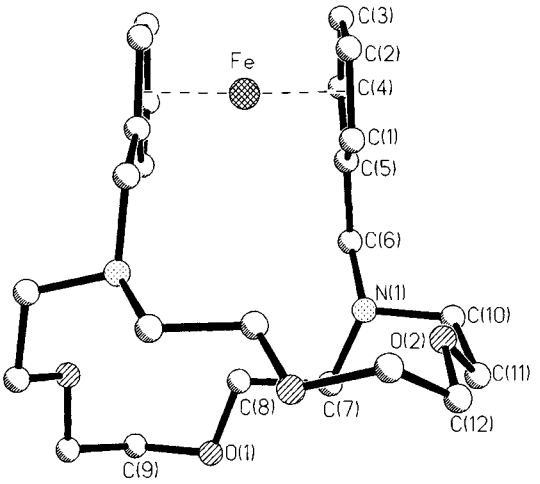

Figure 1. Molecular structure of **5** in the crystal (without hydrogen atoms). Selected bond lengths [pm] and -angles [°]: Cent–Cent′ 330.2(5); C(6)–N(1)–C(7) 111.4(1), C(6)–N(1)–C(10) 109.8(2), C(7)–N(1)–C(10) 112.9(2), N(1)–C(7)–C(8) 110.0(2), C(7)–C(8)–O(1) 109.1(2), C(8)–O(1)–C(9) 113.6(2), C(10)–C(11)–O(2) 108.6(2), N(1)–C(10)–C(11) 114.2(2), C(11)–O(2)–C(12) 113.4(2), C(5)–C(6)–N(1) 113.1(1). Cent and Cent′ denote the two centroids of the two cyclopentadienyl rings

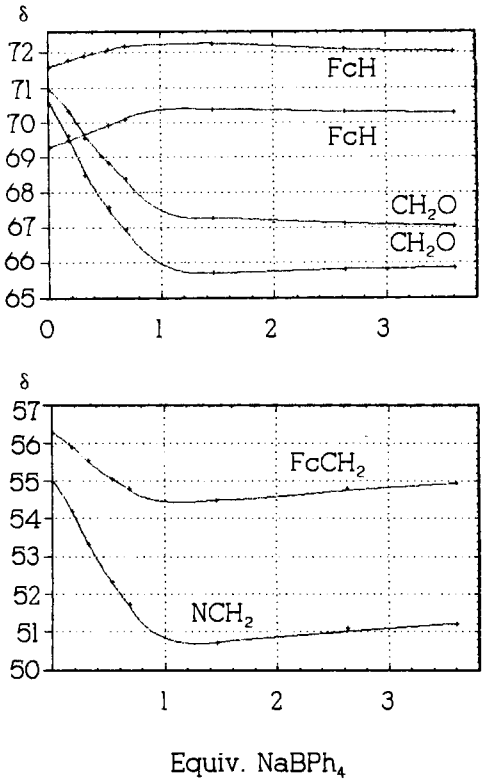

Figure 2. ^{13}C-NMR titration of $Fc(12)_2$ **2** with $NaBPh_4$ in CD_3CN

ppm. A ^{13}C-NMR titration is a quantitative form of this experiment and allows an easy determination of complex stoichiometries in solution. The course of such a titration of $Fc(12)_2$ **2** with $NaBPh_4$ is displayed in Figure 2. Successive additions of $NaBPh_4$ to a CD_3CN solution of **2** cause strong signal shifts only until equimolar amounts of cation and ferrocene are present. Further salt addition of up to 3.6 equivalents has almost no effect on the position of the NMR signals, implying that the 1:1 complex persists in solution.

Addition of Na^+ to the biscrown ethers causes a continuous shift of all NMR signals. This contrasts with the behavior shown by **5**, where addition of Na^+ immediately produces a set of seven new resonances, reflecting the increased kinetic stability of cryptands. Upon further addition these seven lines increase in intensity accompanied by a concomitant decrease of the uncomplexed ferrocene cryptand signals. The large shift differences between the ^{13}C-NMR signals of $Fc(12)_2$ **2** and $Fc(12)_2 \cdot Na^+$ – as compared to **5** and **5** · Na^+ – indicate that the large signal shifts are primarily caused by changes in the conformation of the crown ether and not so much by the positive charge of sodium.

In the same manner as described for $Fc(12)_2$ and Na^+ the complex stoichiometries have been determined for $NaBPh_4$ and $KBPh_4$ with $Fc(15)_2$ **3**. Na^+ forms **3** · 2 $NaBPh_4$, whereas K^+ affords **3** · $KBPh_4$. With lithium, however, the case is much less clear-cut. Thus, additions of lithium ions far beyond reasonable metal-to-ligand ratios produce further shifts. This might be due to the strong polarizing power of Li^+ and renders this technique useless for lithium. The equimolar ratios determined for $Fc(12)_2 \cdot Na^+$ and $Fc(15)_2 \cdot K^+$ suggest the formation of complexes in which the alkali metal is sandwiched between two crown ether rings. The formation of crown ether sandwiches appears likely as the ferrocene sandwich will effect a structural preorganization of the two macrocycles, and the restricted mobility of the cyclopentadienyl rings only permits rotation around the axis linking the two ring centroids and the iron atom. These special structural features have led to ferrocene being described as an atomic ball bearing[13].

NMR spectra of the ferrocene cryptands **5** and **6** with Na^+ have been described recently by Gokel et al.[11] independently of our investigations and will not be discussed here. However, our assignments (based on HETCOR and NOE spectra) of the ^{13}C-NMR resonances disagree (Experimental Section)[14].

Cyclic Voltammetry of 2 and 5 in the Presence of H^+ and Na^+

The most interesting feature of the compounds described here is the combination of electrochemically active ferrocene and cation-binding crown ethers within one molecule. The electrochemistry of the ferrocene/ferrocenium redox couple will directly influence the complexation behavior of the macrocycles. In the neutral form the ferrocene-macrocycle will strongly bind cations; upon oxidation to ferrocenium, however, the unfavorable interaction of two cations in close proximity leads to a destabilization of the complex (Scheme 2). Cyclic voltammetry is a valuable tool to investigate the extent of this redox-switching behavior, which depends on the charge density of the cation, the iron-cation distance, and the stability constant of the cation-macrocycle complex.

Scheme 2. Redox switching and complexation behavior of **5** and Na^+

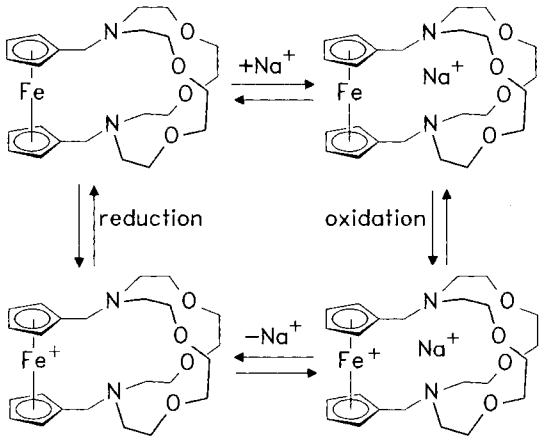

The cyclic voltammogram of $Fc(12)_2$ **2** in CH_3CN/Bu_4NPF_6 displays a redox wave centered at +0.35 V (vs. Ag/AgCl). Stepwise addition of $NaPF_6$ until a 1:1 molar ratio is reached produces a new wave at +0.42 V. The effect of Na^+ addition on the cyclic voltammogram of **5** however is much more pronounced. Addition of substoichiometric amounts of $NaPF_6$ gives a new pair of waves for **5** · Na^+ centered at +0.43 V (vs. Ag/AgCl), which are located at a potential of 180 mV more positive than observed for **5**. The different electrochemical behavior of **2** and **5** is also apparent in the ^{13}C-NMR spectra. Addition of $NaBPh_4$ produces a continuous shift of NMR signals in the case of **2**, whereas for **5** immediately a set of seven new signals is observed. The conclusion drawn from these results emphasizes the strong influence of the iron-sodium distance, the kinetic stability of the crown ether sodium complex and the binding strength of the macrocycle on the redox-switching behavior and the NMR spectra.

In order to better understand the influence of hardness (charge-to-radius ratio) on the electrochemistry of **5** we have investigated the effect of the hardest possible cation: the proton. Stepwise addition of HBF_4 (each step corresponding to 0.2 equivalents of H^+) to an acetonitrile solution of **5** first gives rise to the formation of **5** · H^+, the addition of more acid affords the diprotonated ferrocene-cryptand (Table 1, Figure 3).

The cyclic voltammograms can be divided into three areas, one corresponding to the starting material at +0.25 V, the central one to **5** · H^+, and the one at the most positive potential to **5** · H^+H^+. Monoprotonation gives a new redox wave at +0.47 V (+220 mV relative to **5**). Surprisingly, this shift is intermediate between that of Na^+ (+0.43 V, +180 mV rel. to **5**) and Ca^{2+} addition (+0.52 V, +270 mV rel. to **5**)[11] even though the proton is much harder than both

Table 1. Electrochemical data for the protonation of **5**[a]

H^+/ **5**	E(**5**) [V]	E(**5**•H) [V]		E(**5**•H^+H^+) [V]	
0.0	+0.25	-	-	-	-
0.2	+0.25	+0.47	-	+0.74	-
0.4	+0.25	+0.47	-	+0.74	-
0.8	-	+0.46	+0.6	+0.75	+0.80
1.0	-	+0.47	+0.6	+0.75	+0.83
1.2	-	-	+0.6	-	+0.83
1.6	-	-	-	-	+0.84
1.8	-	-	-	-	+0.85

[a] E (**5**), E (**5** · H) and E (**5** · HH) are the apparent redox potentials of the free ligand (vs. Ag/AgCl), the monoprotonated and the diprotonated ferrocene cryptand. The concentration of the free ligand was $1.17 \cdot 10^{-3}$ M. H^+/(**5**) are the molar ratios of HBF_4 and **5**.

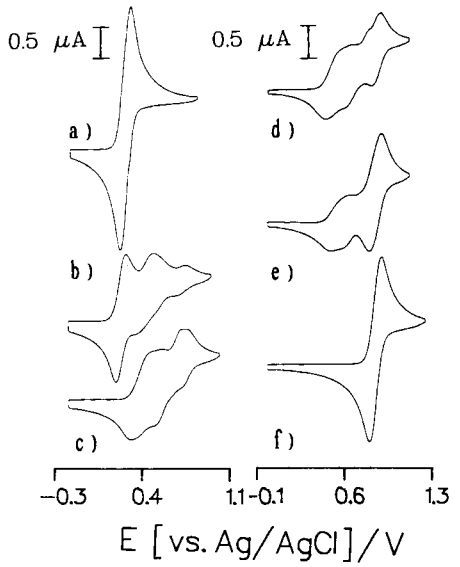

Figure 3. Cyclic voltammograms of the proton titration of **5**. a) **5**, b) +0.4 equiv. of H^+ (HBF_4), c) +0.8 equiv. of H^+, d) +1.0 equiv. of H^+, e) +1.2 equiv. of H^+, f) +2.0 equiv. of H^+ = **5** · H^+H^+. v = 100 mV/s, in CH_3CN/0.1 M $N(C_4H_9)_4PF_6$ (20°C)

the metal ions. This suggests that the iron-proton distance is large. A closer look at the cyclic voltammogram's (Figure 3, d, e) displays an additional wave at a more positive potential of +0.60 V (+350 mV rel. to **5**) in the region of **5** · H^+. Following the addition of 0.4 equivalents of acid (Figure 3b) a new set of redox wave corresponding to **5** · H^+H^+ starts to develop. These waves also results from at least two separate species (Figure 3, c, d), one at +0.75 V (+490 mV rel. to **5**) the other one at +0.85 V (+600 mV rel. to **5**). These large shifts correspond to a reduction of the basicity of **5** by $K_0/K_1 = 5.2 \cdot 10^3$ or $8.2 \cdot 10^6$ [**5**–**5** · H^+)] and $K_0/K_2 = 1.9 \cdot 10^8$ and $1.4 \cdot 10^{10}$ [**5**–**5** · H^+H^+][15].

During protonation at least four different mono- and diprotonated species are formed. Obviously, protonation of a cryptand is a process quite different from the complexation of metal ions. Whereas large metal ions like Na^+ utilize several electron pairs for bonding within the cavity of a macrocycle, the small proton is "coordinated" mainly at the nitrogen lone pair. Crystal structures of protonated cryptands show only weak interactions with neighboring oxygen electron pairs[16,17]. Inversion of the nitrogen changes the relative orientation of the electron pair with respect to the cavity. Consequently, this gives rise to several protonated isomers, which differ with respect to the orientation of the nitrogen lone pair (*exo* or *endo*) (Scheme 3).

Scheme 3. Equilibria for the various protonated forms of **5**

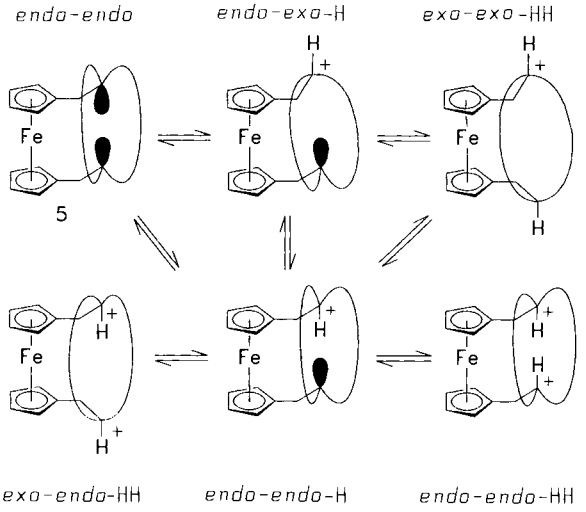

The relative orientation of the three carbon atoms bound to the nitrogen atom in the solid-state structure of **5** shows the typical *endo,endo* orientation of the nitrogen lone pairs, which means that both electron pairs are directed towards the inside of the cavity. This is responsible for the cryptate effect and is crucial for an efficient bonding of large cations. Obviously, the situation for H^+ is different. Inside and outside orientations of the lone pairs give rise to different isomers (Scheme 3). Equilibria of protonated isomers have been investigated in detail for the [1.1.1]cryptand[18]. Whereas the rate constants for the monoprotonation of the [1.1.1]cryptand are already moderate, diprotonation is extremely slow. In 1 M HCl, the second internal protonation requires several weeks at room temperature. Obviously, **5** is not as rigid as the [1.1.1]cryptand. Therefore, the rate constants for protonation will be much higher[19], but as is apparent from the cyclic voltammograms, several protonated species seem to coexist at a given time. Attempts to confirm this independently by ^{13}C-NMR titration experiments have failed due to severe line broadening. This is caused by rapid interconversion between different protonated species. Investigations performed with the [1.1.1]cryptand have shown the *exo*-H isomer to be the kinetically preferred one. The *endo*-H isomer is the product generated under thermodynamic control.

At this point it is difficult to predict which isomer corresponds to which redox potential. However, it looks reasonable to suggest that the isomer with the least positive shift of the redox wave is the one which has the largest separation of the iron atom and the positive charge. As judged from molecular models this should be the *exo*-H^+ isomer. It can now be understood why **5** · Ca^{2+} displays a

more positive redox potential than **5**-*exo*-H^+. Consequently, the wave located at a more positive potential should correspond to the *endo*-H^+ isomer. On the other hand, the species with the most positive potential will have the smallest distance between the iron atom and the positive charge. Therefore, it seems likely that the redox wave at +0.85 V corresponds to the *endo,endo*-H^+H^+ isomer. These assignments appear reasonable on the basis of simple cyclic voltammetry shift arguments. To prove this hypothesis, a detailed investigation of the kinetics and thermodynamics of the protonation of **5** is required.

Conclusion and Outlook

The facile synthesis of ferrocene cryptands and ferrocene crown ethers allowed us to study the protonation equilibria. The protonation of the ferrocene cryptand **5** shifts the redox potential of the ferrocene unit by up to +600 mV, corresponding to a reduction in the basicity of **5** by a factor of $1.4 \cdot 10^{10}$, **5** · H^+H^+ may thus be viewed as a redox-switched acid. Treatment of smaller diaza crown ethers with the ferrocene pyridinium salt **1** allows the synthesis of ferrocene cryptands with smaller cavities for a selective complexation of smaller cations[20]. Their higher charge-to-radius ratio should evoke even larger redox-switching effects. The potential of the ferrocene cryptand **5** and related ferrocenophanes[21] for the active, directed membrane transport of protons is an attractive target for future investigations[22].

We thank the *Deutsche Forschungs-Gemeinschaft* for a Habilitationsstipendium to H.P., the *Wissenschaftliche Gesellschaft Freiburg*, Prof. Dr. *H. Vahrenkamp* for his support and Dipl.-Chem. *U. Hartmann* for the collection of the X-ray data.

Experimental

All reactions were carried out under dry nitrogen using standard Schlenk techniques. Commercially available solvents and reagents were purified according to literature procedures[23]. – Chromatography: Silica MN 60. – NMR: 300 K, Bruker AC 200 F (^{1}H NMR 200 MHz, ^{13}C NMR 50 MHz) or Varian Unity 300 (^{1}H NMR 300 MHz, ^{13}C NMR 75 MHz), referenced to residual protons in $CDCl_3$ (δ = 7.26, 77.0), CD_3CN (1.93, 1.30). – Elemental analyses: Mikroanalytisches Laboratorium der Chemischen Laboratorien Universität Freiburg. – Melting points: Meltemp melting point apparatus in sealed capillaries. – Starting materials were commercially available or prepared according to literature procedures: aza-12-crown-4[24], aza-15-crown-5[25], aza-18-crown-6[25], 1,1′-ferrocenylene-bis(methylenepyridinium) tosylate chloride (**1**)[9].

NMR Titration Experiments: 8–10 mg of the ferrocene crown ethers was dissolved in 0.4 ml of CD_3CN. To these solutions were added stepwise portions of the solid tetraphenylborates or $LiAsF_6$. The exact ratio of ferrocene to cation was determined by integration of the ^{1}H-NMR signals. Usually, less than 400 pulses (ca. 20-min acquisition time) in the ^{13}C NMR (50 MHz) were sufficient to give a reasonable signal-to-noise ratio for the CH_2 and CH carbon atoms, even though substoichiometric amounts of the cation cause line broadening.

Cyclic Voltammetry: The standard electrochemical instrumentation consisted of a PAR Model 173 potentiostat/galvanostat and a PAR Model 175 Universal programmer. Cyclic voltammograms were recorded with a Philips Model PM 8033 X-Y recorder. A three-electrode configuration was employed. The working electrode was a Pt disk (diameter 1 mm) sealed in soft glass. The counter electrode was a Pt wire coiled around the glass mantle of the working electrode. The reference electrode was an Ag wire on which AgCl had been deposited electrochemically. Potentials were calibrated against the formal potential of cobaltocenium perchlorate (−0.94 V vs. Ag/AgCl). NBu_4PF_6 was used as a supporting electrolyte.

1,1′-Ferrocenylene-bis(methylene-aza-x-crown-y) [*x*/*y* = 12/4 (**2**); 15/5 (**3**); 18/6 (**4**)]: Mixtures of 1,1′-ferrocenylene-bis(methylenepyridinium) tosylate chloride (**1**) (5.77 g, 10 mmol), monoaza-crown (12/4 = 3.5 g or 15/5 = 4.4 g or 18/6 = 5.3 g, 20 mmol), and Na_2CO_3 (4.23 g, 40 mmol) were heated to reflux in 75 ml acetonitrile for 12 h. After filtration the volatile compounds were removed in vacuo, to the residues was added 10 ml of water, and the product was extracted two times with 50 ml CH_2Cl_2. The organic layers were separated, dried with $MgSO_4$ and the CH_2Cl_2 evaporated. The residues were purified chromatographically (cyclohexane/ethylacetate/diethylamine) to afford the biscrown ethers **2**, **3**, and **4** in yields of 45–55%.

2: Yellow-orange solid. – ^{1}H NMR ($CDCl_3$, 200 MHz): 2.61 (t, *J* = 4.8 Hz, 8H, NCH_2), 3.51–3.56 (m, 12H), 3.63 (m, 16H), 4.01–4.03 (m, 8H, FcH). – ^{13}C NMR ($CDCl_3$, 75 MHz): δ = 53.92 (NCH_2), 55.63 ($FcCH_2$), 68.43 (FcH), 69.87 (CH_2O), 70.40 (CH_2O), 70.58 (FcH), 71.05 (CH_2O), 83.12 (Fc). – ^{13}C NMR (CD_3CN): δ = 55.00, 56.28, 69.30, 70.53, 70.96, 71.60, 85.08. – $C_{28}H_{44}FeN_2O_6$ (560.5): calcd. C 60.0, H 7.85; found C 59.7, H 7.90.

3: Orange-red oil. – ^{1}H NMR (200 MHz, $CDCl_3$): δ = 2.67 (t, *J* = 5.9 Hz, 8H, NCH_2), 3.51–3.65 (m, 36H), 4.00–4.04 (m, 8H, FcH). – ^{13}C NMR (50 MHz, $CDCl_3$): δ = 53.51 (NCH_2), 55.78 ($FcCH_2$), 68.53 (FcH), 69.74, 70.07, 70.39, 70.62, 70.94, 83.16 (Fc). – $C_{32}H_{52}FeN_2O_8$ (648.6): calcd. C 59.3, H 8.08; found C 58.9, H 8.21.

4: Yellow-orange solid. – ^{1}H NMR (200 MHz, $CDCl_3$): δ = 2.66 (t, *J* = 5.8 Hz, 8H), 3.50–3.66 (m, 44H), 3.99–4.03 (m, 8H). – ^{13}C NMR (50 MHz, $CDCl_3$): δ = 53.03 (NCH_2), 54.86 ($FcCH_2$), 68.43 (FcH), 69.72, 69.85, 70.57, 70.65, 70.69, 70.75, 83.04 (Fc). – $C_{36}H_{60}FeN_2O_{10}$ (736.7): calcd. C 58.7, H 8.21; found C 58.5, H 8.08.

1,1′-Ferrocenylene-[bis-7,16-methylene(1,4,10,13-tetraoxa-7,16-diazacyclooctadecane)] (**5**) *and 1,1″:1′,1‴-Bisferrocenylene-bis[bis-7,16-methylene(1,4,10,13-tetraoxa-7,16-diazacyclooctadecane)]* (**6**): A mixture of **1** (2.31 g, 4.0 mmol), Na_2CO_3 (0.85 g, 8 mmol), and 1,4,10,13-tetraoxa-7,16-diazacyclooctadecane (1.03 g, 4.0 mmol) in 80 ml of acetonitrile was heated to reflux for 12 h, the cold solution filtered and the volatile compounds evaporated in vacuo. Then 5 ml of water was added to the residue and the product extracted three times with 25 ml of CH_2Cl_2. The combined organic layers were dried with $MgSO_4$ and the CH_2Cl_2 evaporated. The residue was purified chromatographically (cyclohexane/ethylacetate/diethylamine) to afford the ferrocene cryptands **5** and **6** in slightly variable yields of 55% (**5**) and 15% (**6**).

5: Yellow solid, m.p. 118°C. – ^{1}H NMR (300 MHz, $CDCl_3$): δ = 2.53 (m, 4H, OC*H*H), 2.69 (m, 4H, OCH*H*), 3.60 (m, 16H, $FcCH_2$ + OCH_2), 3.73 (m, 4H, OCH*H*), 3.99 ('t', *J* = 1.8 Hz, 4H, 3-FcH), 4.23 ('t', *J* = 1.8 Hz, 4H, 2-FcH). – ^{13}C NMR (75 MHz, CD_3CN): δ = 54.32 ($FcCH_2$), 55.37 (NCH_2), 67.51 (3-FcH), 70.57 (2-FcH), 70.81 (CH_2O), 71.41 (CH_2O), 89.31 (Fc).

6: ^{1}H NMR (200 MHz, $CDCl_3$): δ = 2.74 (t, *J* = 5.5 Hz, 16H, NCH_2), 3.59–3.65 (m, 40H, $FcCH_2$ + CH_2O), 4.05–4.15 (m, 16H, FcH). – ^{13}C NMR (50 MHz, $CDCl_3$): δ = 53.29 (NCH_2), 54.01 ($FcCH_2$), 68.34 (FcH), 69.50 (CH_2O), 70.69 (CH_2O), 70.73 (FcH), 83.54 (Fc).

Salts of **2**, **3**, *and* **5** *with* $NaBPh_4$ *and* $KBPh_4$: The respective salts were prepared by combining solutions of **2**, **3**, or **5** in acetonitrile with $NaBPh_4$ or $KBPh_4$ in the same solvent in the required stoichiometries as determined by NMR titration experiments. NMR data (200 MHz, CD_3CN) are only listed for the cations, BPh_4^- resonances not given. **2** · $NaBPh_4$: ^1H NMR: $\delta = 2.53$ (t, $J = 4.6$ Hz, 8H, NCH_2), 3.55 (t, $J = 4.6$ Hz, 8H, OCH_2), 3.64 (s, 16H, OCH_2), 3.80 (s, 4H, $FcCH_2$), 4.19 (s, 8H, FcH). – ^{13}C NMR: $\delta = 50.46$ (NCH_2), 54.32 ($FcCH_2$), 65.51 (OCH_2), 66.23 (OCH_2), 67.25 (OCH_2), 70.41 (FcH), 72.35 (FcH), 80.97 (Fc).

3 · 2 $NaBPh_4$: ^1H NMR: $\delta = 2.49$ (t, $J = 4.8$ Hz, 8H, NCH_2), 3.48 (t, $J = 4.8$ Hz, 8H, CH_2O), 3.58–3.62 (m, 28H, CH_2O + $FcCH_2$), 4.11–4.15 (m, 8H, FcH). – ^{13}C NMR: $\delta = 52.75$ ($FcCH_2$), 53.11 (NCH_2), 67.57 (CH_2O), 68.95 (CH_2O), 69.47 (CH_2O), 70.15 (FcH), 72.21 (FcH), 81.38 (Fc).

5 · $NaBPh_4$: ^1H NMR: $\delta = 2.59$–2.67 (m, 8H, NCH_2), 3.42 (s, 4H, $FcCH_2$), 3.58 (OC*H*H), 3.68 (C*H*HO), 3.61 (CH*H*O), 3.81 (OCH*H*), 4.15 ('t', $J = 1.9$ Hz, FcH), 4.26 ('t', $J = 1.9$ Hz, FcH). – ^{13}C NMR: 54.57 ($FcCH_2$), 56.25 (NCH_2), 67.99 (FcH), 68.14 (CH_2O), 69.66 (FcH), 70.24 (CH_2O), 88.04 (Fc). – ^{23}Na NMR (78.5 MHz, D_2O vs. ext. 1 m M NaCl/D_2O): $\delta = -6.7$.

5 · $KBPh_4$: ^1H NMR: $\delta = 2.60$ (br, 8H, NCH_2), 3.46 (br, 4H, $FcCH_2$), 3.63 (m, CH_2O), 3.65 (C*H*HO), 3.75 (CH*H*O), 4.15 ('t', $J = 1.9$ Hz, FcH), 4.35 (br, FcH). – ^{13}C NMR: $\delta = 52.98$ ($FcCH_2$), 57.01 (NCH_2), 68.08 (CH_2O), 68.29 (FcH), 68.95 (FcH), 70.51 (CH_2O), 88.10 (Fc).

X-Ray Crystal Structure Determination of **5**: Crystals of **5** were grown by slowly cooling a toluene/hexane solution. X-ray data were collected on an Enraf-Nonius CAD4 by using a graphite monochromator and Mo-K_α radiation (71.073 pm). Crystal dimensions: red cubes 0.5 × 0.4 × 0.3 mm. Formula: $C_{24}H_{36}FeN_2O_4$ (472.4). Space group: monoclinic *C*2/*c*. Cell dimensions: $a = 17.922(4)$, $b = 9.490(2)$, $c = 14.548(3)$ pm, $\beta = 111.64(3)°$, $V = 2299.9(9)$ Å, $Z = 4$. $F(000) = 1008$. Density: 1.364 gcm^{-3}. Absorption coefficient: 0.688 mm^{-1}. Extinction coefficient: 0.0079(7). An empirical absorption correction (psi scans) and an extinction correction were applied. Scan type: ω-2ϑ. ϑ-range: 2.5–26°. Index range: h −22–0, k −11–0, l −16–+18, number of reflections (collected, independent, observed): 2407, 2333 ($R_{int.} = 0.055$), 2128 ($4\sigma F$). Number of parameters: 142. Final R indices [$2\sigma(I)$]: $R_1 = \sigma \mid F_o - F_c \mid / \sigma(F_o) = 3.17\%$, $wR_2 = \{\sigma[w(F_o^2 - F_c^2)^2]/\sigma[w(F_o^2)^2]\}^{0.5} = 9.10\%$. GooF $[\sigma[w(F_o^2 - F_c^2)^2]/(n - p)]^{0.5} = 1.09$. Min. and max. residual electron density [eÅ^{-3}]: +0.51, −0.23. Systematic absence indicated either *Cc* or *C*2/*c*. The structure was solved in *C*2/*c* with direct methods and refined by full-matrix least-squares[26,27] against F^2. All non-hydrogen atoms were refined with anisotropic thermal parameters. All hydrogen atoms were localized and refined with fixed isotropic temperature coefficients[28].

[1] F. G. A. Stone, G. Wilkinson, E. W. Abel (Eds.), *Comprehensive Organometallic Chemistry*, Pergamon Press, London, **1982**.
[2] B. Dietrich, P. Viout, J. M. Lehn, *Macrocyclic Chemistry*, VCH Weinheim, **1993**; S. R. Cooper (Ed.), *Crown Compounds*, VCH Weinheim, **1992**; S. Patai, Z. Rappoport (Eds.), *Crown Ethers and Analogs*, Update from Chemistry of functional Groups, J. Wiley et Sons, Chichester, **1989**.
[3] F. Vögtle, *Supramolekulare Chemie*, F. Teubner Verlag, Stuttgart, **1989**.
[4] P. D. Beer, *Chem. Soc. Rev.* **1989**, *18*, 409; S. Akabori, Y. Habata, Y. Sakamoto, M. Sato, S. Ebine, *Bull. Chem. Soc. Jpn.* **1983**, *56*, 537; G. DeSantis, L. Fabrizzi, M. Licchelli, P. Pallavicini, A. Perotti, *J. Chem. Soc., Dalton Trans.* **1992**, 3283; I. Bernal, E. Raabe, G. M. Reisner, R. A. Bartsch, R. A. Holwerda, B. P. Czech, Z. Huang, *Organometallics* **1988**, *7*, 247.
[5] P. D. Beer, A. D. Keefe, H. Sikanyika, C. Blackburn, J. F. McAleer, *J. Chem. Soc., Dalton Trans.* **1990**, 3289.
[6] C. D. Hall, N. W. Sharpe, I. P. Danks, Y. P. Sang, *J. Chem. Soc., Chem. Commun.* **1989**, 419.
[7] M. C. Grossel, M. R. Goldspink, J. A. Hriljac, S. C. Weston, *Organometallics* **1991**, *10*, 851.
[8] C. D. Hall, J. H. R. Tucker, A. Sheridan, S. Y. F. Chu, D. J. Williams, *J. Chem. Soc., Dalton Trans.* **1992**, 3133.
[9] V. P. Tverdokhlebov, I. V. Tselinskii, B. V. Gidaspov, G. Y. Chikisheva, *J. Org. Chem. (U.S.S.R)* **1976**, *12*, 2268 (Engl. Transl.).
[10] G. Oepen, F. Vögtle, *Liebigs Ann. Chem.* **1979**, 1094.
[11] Independently of our own work, Gokel et al. have recently published related work on Na^+ and K^+ complexes of **5** and **6**. J: C. Medina, T. T. Goodnow, M. T. Rojas, J. L. Atwood, B. C. Lynn, A. C. Kaifer, G. W. Gokel, *J. Am. Chem. Soc.* **1992**, *114*, 10583.
[12] M. Herceg, R. Weiss, *Bull. Chim. Soc. Fr.* **1972**, 549.
[13] G. W. Gokel, J. C. Medina, C. Li, *Synlett* **1991**, 677; J. C. Medina, C. Li, S. G. Bott, J. L. Atwood, G. W. Gokel, *J. Am. Chem. Soc.* **1991**, *113*, 366; E. C. Constable, *Angew. Chem.* **1991**, *103*, 418; *Angew. Chem. Int. Ed. Engl.* **1991**, *30*, 407.
[14] In ref.[11] the assignment of the peaks in the ^{13}C-NMR spectrum of **5** is based on spectra recorded in $CDCl_3$ solution. These assignments were erroneously also used for the ^{13}C spectra of the metal ion complexes of **5** even though they were recorded in CD_3CN.
[15] S. R. Miller, D. A. Gustowski, Z. Chen, G. W. Gokel, L. Echegoyen, A. E. Kaifer, *Anal. Chem.* **1988**, *60*, 2021; C. Elschenbroich, S. Hoppe, B. Metz, *Chem. Ber.* **1993**, *126*, 399.
[16] B. G. Cox, J. Murray-Rust, N. Murray-Rust, N. van Truong, H. Schneider, *J. Chem. Soc., Chem. Commun.* **1982**, 377.
[17] H. Brügge, K. Carboo, A. von Deuten, A. Knöchel, J. Kopf, W. Dreissig, *J. Am. Chem. Soc.* **1986**, *108*, 107.
[18] J. Cheney, J. P. Kintzinger, J. M. Lehn, *Nouv. J. Chim.* **1978**, *2*, 411.
[19] P. B. Smith, J. L. Dye, J. Cheney, J. M. Lehn, *J. Am. Chem. Soc.* **1981**, *103*, 6044.
[20] H. Plenio, R. Diodone, work in progress.
[21] H. Plenio, publication in preparation.
[22] B. G. Malmström, *Acc. Chem. Res.* **1993**, *26*, 332.
[23] D. D. Perrin, W. L. Armarego, *Purification of Laboratory Chemicals*, 3rd ed., Pergamon Press, Oxford, U.K., **1988**.
[24] M. J. Calverly, J. Dale, *Acta Chim. Scand., Ser. B*, **1982**, *36*, 241.
[25] H. Maeda, S. Furuyoshi, Y. Nakatsuji, M. Okahara, *Bull. Chem. Soc. Jpn.* **1983**, *56*, 212.
[26] G. M. Sheldrick, *SHELXS 86*, Universität Göttingen, **1990**.
[27] G. M. Sheldrick, *SHELXL 93*, Universität Göttingen, **1993**.
[28] Further details of the crystal structure investigation are available on request from the Fachinformationszentrum Karlsruhe, Gesellschaft für wissenschaftlich-technische Information mbH, D-76344 Eggenstein-Leopoldshafen, on quoting the depository number CSD-400211, the names of the authors, and the journal citation.

[188/93]